Progress In Electromagnetics Research Letters, Vol. 3, 25–33, 2008

ANALYSIS OF CAPACITIVELY COUPLED MICROSTRIP-RING RESONATOR BASED ON SPECTRAL DOMAIN METHOD

R. Rezaiesarlak and F. Hodjatkashani

Department of Electrical Engineering
Iran University of Science & Technology
Tehran, Iran

E. Mehrshahi

Department of Electrical Engineering
Shahid Beheshti University
Tehran, Iran

Abstract—In this paper, full-wave analysis of a microstrip-ring resonator capacitively coupled to Microstrip transmission line is presented. The method of the analysis is based on spectral domain in rectangular coordinate system. Since this coordinate system is not compatible with ring structure, triangular basis functions have been utilized for the current distributions on the ring surface. Applying Galerkin's method in spectral domain, the resonant frequencies of the structure and current distributions on the conductors are calculated and the effects of various parameters are studied. To verify the method of analysis, our results are compared with others and the accuracy of the method has been confirmed.

1. INTRODUCTION

Compact size, low cost, high Q and low radiation loss are the desired features of microstrip ring resonator. It has been used for the measurement of dispersion, phase velocity [1–3], dielectric constant [4], discontinuities [5, 6] and other special applications [7]. This structure is also used for designing microstrip filters [8–10]. The interest of researchers and commercial communication industry engineers to these structures has recently increased due to the application of ferroelectric thin-film substrates, high-temperature superconducting microstrip lines and metamaterials in ring resonator fabrication [11–14]. Because of this wide range of applications, many researches have been made to analyze these structures [1, 15–19]. But in the previous works, the method of analysis was based on Hankel Transform Method (HTM) without considering feeding line. In [16], the analysis of microstrip ring resonator considering probe excitation is presented and in [17–19], the analysis of ring resonator coupled to feeding line is presented by making the use of FDTD [17, 18] and ABCD and Y-admittance matrices [19]. In this paper, using the moment method in the spectral domain, full wave analysis of the structure is presented. We've utilized appropriate basis functions for the currents on the conductors which are analytically Fourier transformable. By applying Galerkin's method in the spectral domain, the currents on the conductors, coupling between microstrip and ring resonator and the resonant frequencies of the structure are obtained.

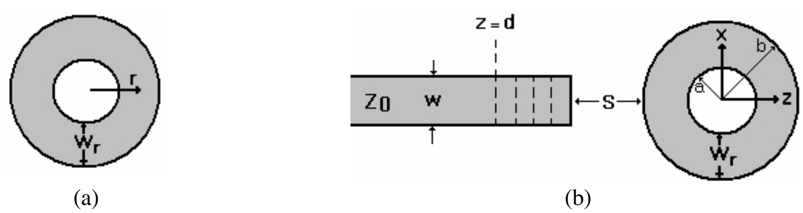

Figure 1. (a) The microstrip ring resonator that locates above the dielectric substrate. (b) Capacitively coupled microstrip-ring resonator.

2. THE METHOD OF ANALYSIS

Figure 1(a) shows the schematic view of a microstrip ring resonator without any feeding line around it. If the inner and outer radiuses of the isolated ring resonator do not differ so much from each other, the microstrip ring may have the same dispersion characteristics as those for the linear one. Thus, it can be analyzed by viewing it as a microstrip line that ends on itself [1]. The resonant frequencies correspond to a condition where the perimeter of the ring is an integer multiple of the guided wavelength. That is,

$$2\pi r = n\lambda_g \qquad n = 1, 2, \ldots \tag{1}$$

where r is the average radius of ring and λ_g is the function of microstrip parameters. As the line is located around the ring, the resonant frequencies are shifted as a small value. As Fig. 1(b) shows, a Z_0-microstrip line has been coupled to the microstrip ring resonator. To analyze this structure, it is assumed that waves are lunched from $z = -\infty$. The currents on the line are propagated towards the ring, until they arrive at the end of the line. At this point reflection is occurred and near this discontinuity, the currents are affected by the excitation of high order modes. If β is considered as a propagation constant of the line along the z-direction and $f_x(x)$ and $f_z(x)$ are the x and z-directed currents on the uniform and infinitely line with the same dimensions, then the currents on the line in Fig. 1(b) can be written in the spatial domain as below

$$J_x^{Line}(x,z) = f_x(x)\cdot\left[\left(e^{-j\beta(z-d)} - \Gamma\cdot e^{j\beta(z-d)}\right) + \sum_m a_m^x g_m(z)\right] \quad \text{(2a)}$$

$$J_z^{Line}(x,z) = f_z(x)\cdot\left[\left(e^{-j\beta(z-d)} + \Gamma\cdot e^{j\beta(z-d)}\right) + \sum_m a_m^z g_m(z)\right] \quad \text{(2b)}$$

where $g_m s$ are PSW-P basis functions. To obtain propagation constant and transverse currents in (a), the Standard spectral domain method [19, 20] or the immittance approach [21] can be utilized. To accommodate high variations in the ring surface, the currents on the ring are expanded versus triangular basis functions as bellow

$$J_x^{Ring}(x,z) = \sum_{m,n} c_{mn} J_x^{mn}(x,z) \quad \text{(2c)}$$

$$J_z^{Ring}(x,z) = \sum_{m,n} d_{mn} J_z^{mn}(x,z) \quad \text{(2d)}$$

Since our analysis is based on spectral domain method, we should apply 2-dimensional Fourier transform into (2). This Fourier transform is defined as

$$\tilde{F}(k_x,k_z) = \int_z \int_x f(x,z)\cdot \exp(jk_x x + jk_z z)dx\cdot dz \quad \text{(3)}$$

The significant point in this process is that, the basis functions are selected which the integrals in (3) can been analytically solved.

3. BASIS FUNCTIONS

In the microstrip line regions far from discontinuity full domain basis functions $f_x(x)$ and $f_z(x)$ are used to satisfy edge conditions and also to provide fast convergence. These functions are Maxwellian type functions defined in [20, 22]. In the perturbed regions, however, pulse and PSW-S sub-sectional basis functions (g_m^x and g_m^z), discussed in [23], are used to accommodate possible high variations in the current distributions and also to add flexibility to the structure configuration. For currents on the ring resonator as defined in (2b), (2c), triangular basis functions have been utilized as shown in Fig. 2. These functions are defined as

$$S(x,z) = \begin{cases} 1 & (x,z) \in \Sigma \\ 0 & \text{otherwise} \end{cases} \tag{4}$$

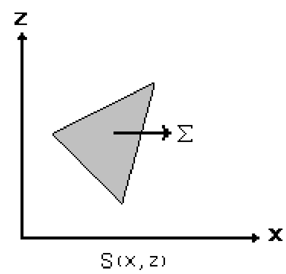

Figure 2. Triangular basis function.

4. SPECTRAL DOMAIN APPROACH

By satisfying boundary conditions in Fig. 1(b), tangential electric fields on the conductors at $y = h$ can be written versus currents on the line and the ring resonator in the spectral domain as bellow [20]

$$\begin{bmatrix} \tilde{E}_x(k_x,k_z) \\ \tilde{E}_z(k_x,k_z) \end{bmatrix} = \begin{bmatrix} \tilde{Z}_{xx} & \tilde{Z}_{xz} \\ \tilde{Z}_{zx} & \tilde{Z}_{zz} \end{bmatrix} \begin{bmatrix} \tilde{J}_x(k_x,k_z) \\ \tilde{J}_z(k_x,k_z) \end{bmatrix} \tag{5}$$

where

$$\begin{aligned} \tilde{Z}_{xx} &= \frac{-1}{k_x^2+\beta^2}\left[\beta^2 \cdot \tilde{Z}_h + k_x^2 \cdot \tilde{Z}_e\right] \\ \tilde{Z}_{xz} &= \tilde{z}_{zx} = \frac{-k_x\beta}{k_x^2+\beta^2}\left[\tilde{Z}_e - \tilde{Z}_h\right] \\ \tilde{Z}_{zz} &= \frac{-1}{k_x^2+\beta^2}\left[k_x^2 \cdot \tilde{Z}_h + \beta^2 \cdot \tilde{Z}_e\right] \\ \tilde{Z}_e &= \frac{j\omega\mu}{\gamma_2 + \gamma_1 \coth \gamma_1 h} \end{aligned}$$

$$\tilde{Z}_h = -\frac{j\gamma_1}{\omega\varepsilon \times \left(\frac{\varepsilon_0\gamma_1}{\varepsilon_r\gamma_2} + \coth(\gamma_1 h_1)\right)}$$

$$\gamma_1 = \sqrt{k_x^2 + \beta^2 - \omega^2\mu\varepsilon_r}$$
$$\gamma_2 = \sqrt{k_x^2 + \beta^2 - \omega^2\mu\varepsilon_0}$$

After substituting Fourier transforms of the currents into (5), one takes inner products of the equations in (12) with the known basis functions using Parseval's theorem, this process yield the matrix equation.

$$\left[\tilde{M}\right][X] = \left[\tilde{M}\right]\begin{bmatrix}[\Gamma]\\ [a]\\ [c]\\ [d]\\ [e]\\ [f]\end{bmatrix} = \left[\tilde{V}\right] \tag{6}$$

where $[X]$ indicates the coefficients of basis functions in (2). By equaling the determinant of $\tilde{M}$ by zero, the resonant frequencies of the structure are determined.

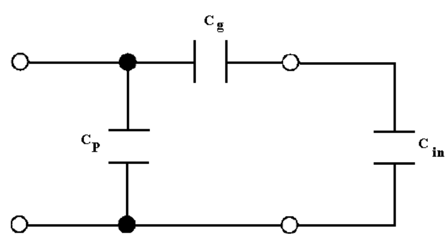

Figure 3. Equivalent circuit of the structure.

5. THE EQUIVALENT CIRCUIT OF THE STRUCTURE

In the pervious section, the analysis of the structure was described. Before representing the numerical results, we would like to present the equivalent circuit of the structure. This circuit should model the effects of various parameters on the frequency responses. Fig. 3 shows the equivalent circuit of the structure. In this circuit, ring is modeled by C_{in} that could be approximated by the transmission line modeling as

$$C_{in} = \frac{2Y_r(1 - \cos(\beta_r l))}{\sin(\beta_r l)} \quad (7)$$

where Y_r = characteristics impedance of the line, β_r = Propagation constant of the line and $l = 2\pi r$ [19]. C_g is in consequence of coupling between the line and ring in gap region and C_P is caused by the fringing fields near the coupling region.

6. NUMERICAL RESULTS

In order to validate the presented formulation, consider the structure shown in Fig. 1(b) with these parameters: Dielectric constant (ε_r) = 2.2, substrate thickness (h) = 0.7874 mm, W = 2.3495 mm, b = 11.47 mm, S = 0.9 mm. Fig. 4 shows the first resonant frequency of the structure shown in Fig. 1(a) versus the inner radius of the ring (a). According to this figure, the first resonant frequency of the ring is decreased as the a (inner radius) approach to b (outer radius). Now, by locating the microstrip transmission line besides the ring, As the coupling between the ring and microstrip line is achieved, addition to the series resonance (f_S), a parallel resonance (f_P) is appeared. As the gap is decreased and therewith the coupling is intensified, the difference between these two resonances is also increased. Therefore, $|f_P - f_S|$ is in proportion of coupling. In Fig. 5, the fundamental frequencies of the structure with $W = W_r$ versus gap size are shown. Our results are compared by the method of transmission line modeling in [19].

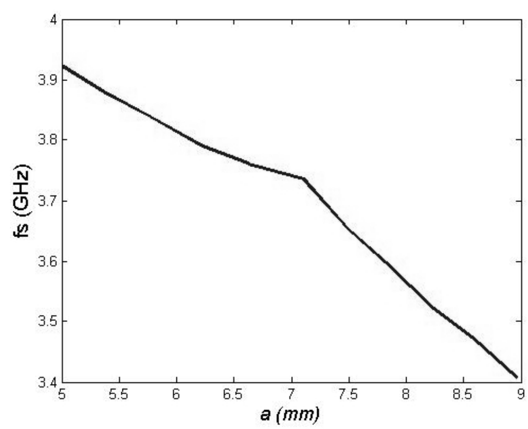

Figure 4. The first resonant frequency of the structure in Fig. 1(a) versus the inner radius of the ring (a).

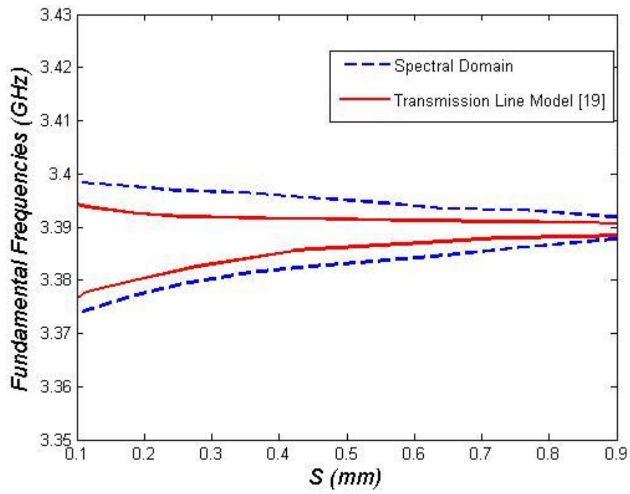

Figure 5. Fundamental frequencies versus gap size are shown and the results of our analysis are compared by [19].

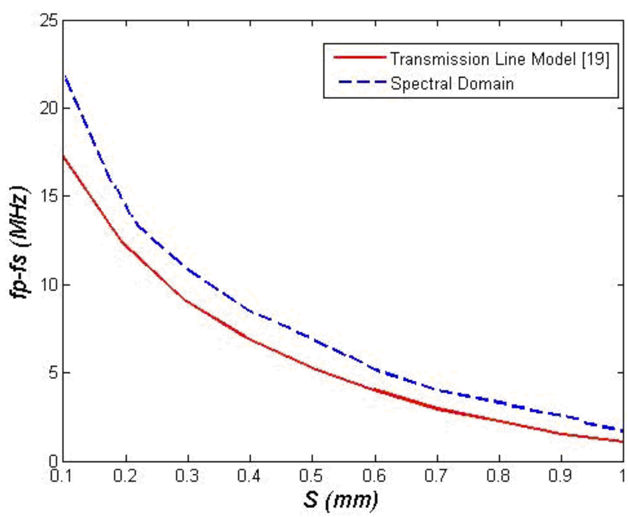

Figure 6. Difference between the theoretical series and parallel resonant frequencies as a function of coupling gap size.

In Fig. 6, the difference between the theoretical series and parallel resonant frequencies as a function of coupling gap sizes is shown.

7. CONCLUSION

In this paper, using appropriate basis functions that were anatically Fourier transformable, we could present full wave analysis of the microstrip ring resonator that capasitively coupled to microstrip line. As the coupling is increased, the distance between series and parallel frequencies is increased. This paper could be useful in designing microstrip filters and resonators.

REFERENCES

1. Chang, K., *Microwave Ring Circuits and Antennas*, John Wiley & Sons, 1996.
2. Wolff, I. and N. Koppik, "Microstrip ring resonator and dispersion measurement on microstrip lines," *Electron Lett.*, Vol. 7, No. 26, 779–781, Dec. 1971.
3. Edwards, C., "Microstrip measurements," *IEEE MTT-S Int. Microwave Symp. Dig.*, 338–341, Dallas, TX, 1982.
4. Bernard, P. A. and J. M. Gautray., "Measurement of dielectric constant using a microstrip ring resonator," *IEEE Trans. Microwave Theory Tech.*, Vol. 39, 592–595, 1991.
5. Stephenson, I. M. and B. Easter, "Resonant techniques for establishing the equivalent circuits of small discontinuities in microstrip," *Electron Lett.*, No. 7, 582–584, 1971.
6. Hoefer, W. J. R. and A. Chattopadhyay, "Evaluation of the equivalent circuit parameters of microstrip discontinuities through perturbation of a resonant ring," *IEEE Trans. Microwave Theory Tech.*, Vol. 23, 1067–1071, 1975.
7. Sarabandi, K. and E. S. Li, "Microstrip ring resonator for soil moisture measurements," *IEEE Trans. Microwave Theory Tech.*, Vol. 35, No. 5, 1997.
8. Wu, Q. S, Q. Xue, and C. H. Chan, "Bandpass filter using microstrip ring resonators," *Electron. Lett.*, Vol. 39, No. 1, 62–64, 2003.
9. Jovanovic, S. and A. Nesic, "Microstrip bandpass filter with new type of capacitive coupled resonator," *Electronic Letters*, Vol. 41, No. 1, 12–13. 2005.
10. Prabhu, S. and J. S. Mandeep, "Microstrip bandpass filter at S-band using capacitive coupled resonator," *Progress In Electromagnetics Research*, PIER 76, 223–228, 2007.
11. Bhasin, K. B., C. M. Chorey, J. D. Warner, R. R. Romanofsky, V. O. Heinen, K. S. Kong, H. Y. Lee, and T. Itoh, "Performance

and modeling of superconducting ring resonators at millimeter-wave frequencies," *IEEE MTT-S Int. Microwave Symp. Dig.*, Part 1, Vol. 1, 269–272, Dallas, TX, 1990.
12. Miranda, A., F. W. van Keuls, R. R. Romanofsky, and G. Subramanyam, "Tunable microwave components for Ku and K-band satellite communications," *Proc 10th Int. Symp. Integrated Ferroelectron*, Part 2, Vol. 22, 269–278, Monterey, CA, 1998.
13. Allen, C. A., K. M. K. H. Leong, and T. Itoh, "Dual-mode composite-right/left-handed transmission line ring resonator," *Electron Lett.*, Vol. 42, 2006.
14. Lee, S. W., Y. Kuga, and A. Ishimaru, "Quasi-static analysis of metamaterials with small tunable stacked split ring resonators," *Progress In Electromagnetics Research*, PIER 51, 219–229, 2005.
15. Sharma, A. K. and B. Bhat, "Spectral domain analysis of microstrip ring resonators," *AEU*, Vol. 33, 130–132, 1979.
16. Ali, S., W. C. Chew, and J. A. Kong, "Vector hankel transform analysis of annular-ring microstrip antenna," *IEEE Trans. on Antenna and Propagation*, Vol. 30, No. 4, July 1982.
17. Semouchkina, E., W. Cao, R. Mittra, and W. Yu, "Analysis of resonance processes in microstrip ring resonators by the FDTD method," *Microw. and Opt. Techn. Lett.*, Vol. 28, No. 5, 2001.
18. Semouchkina, E., W. Cao, and R. Mittra, "Modeling of microwave ring resonator using the finite-difference-time-domain (FDTD) method," *Microw. and Opt. Techn. Lett.*, Vol. 24, No. 6, 2000.
19. Yu, C. C. and K. Chang, "Transmission-line analysis of a capacitively coupled microstrip-ring resonator," *IEEE Trans. Microwave Theory Tech.*, Vol. 45, No. 11, 1997.
20. Itoh, T., *Numerical Techniques for Microwave and Millimeter-Wave Passive Structures*, Wiley, New York, 1989.
21. Itoh, T., "Spectral domain immitance approach for dispersion characteristics of generalized printed transmission lines," *IEEE Trans. Microwave Theory Tech.*, Vol. 8, No. 7, 733–736, 1980.
22. Tran, A. M., B. Houshmand, and T. Itoh, "Analysis of electromagnetic coupling through a thick aperture in multilayer planar circuits using the extended spectral domain approach and finite difference time-domain method," *IEEE Trans. Microwave Theory Tech.*, Vol. 43. No. 9, 1995.
23. Wu, S. C., H. Y. Yang, N. G. Alexopoulos, and I. Wolf, "A rigorous dispersive characteristization of microstrip cross and T junction," *IEEE Trans. Microwave Theory and Thech.*, Vol. 38, No. 12, 1990.